Multispectral pixel performance using a one-dimensional photonic crystal design

X. C. Sun, J. J. Hu, C. Y. Hong, J. F. Viens, X. M. Duan, R. Das, A. M. Agarwal,[a] and L. C. Kimerling
Microphotonics Center, Massachusetts Institute of Technology, Bldg. 13-4118, 77 Massachusetts Avenue, Cambridge, Massachusetts 02139

(Received 14 September 2006; accepted 21 October 2006; published online 1 December 2006)

A photodetector pixel using a photonic crystal structure incorporating photoconductive layers has been realized. The fabricated device exploits mode discrimination and resonant cavity enhancement to provide simultaneous multispectral detection capability, high quantum efficiency, and dramatically suppressed shot noise. Detectivities as high as 2.6×10^{10} and 2.0×10^{10} cm $Hz^{1/2}$ W^{-1} at the two preselected wavelengths, 632 and 728 nm, were achieved, respectively. © *2006 American Institute of Physics*. [DOI: 10.1063/1.2400069]

Applications such as multichemical detection, biological sensing, multispectral imaging, and spectroscopy call for specialized photodetectors that are capable of selectively sensing specific wavelengths simultaneously, namely, multispectral photodetection. Traditionally, multispectral capability has been achieved by several methods, including spatial registration (color filter array),[1,2] temporal registration (mechanical filter wheel),[3] tandem structure,[4] and quantum well photodetectors.[5,6] The first two methods complicate the pixel design and raise the issue of system reliability. In a tandem detector, the top detector serves as a passband filter for the bottom detector. The problem associated with this design is that only certain spectral bands are accessible due to limited material choices. Despite their high leakage current, quantum well detectors are capable of multispectral detection by varying the applied bias. However, the time multiplexing involved prohibits simultaneous detection of different wavelengths, within a single pixel.[7] In addition, all the aforementioned methods necessitate the engineering of lattice-matched single-crystalline materials in order to reduce dark current, which requires high-cost and complicated material growth facilities such as molecular beam epitaxy and metal-organic chemical vapor deposition.

In this letter, we present a designed and fabricated photonic crystal structure incorporating photoconductive layers to achieve simultaneous multispectral detection. This photoconductor pixel exploits resonant cavity enhancement (RCE) for multispectral capability, high quantum efficiency, and dramatically suppressed shot noise. As we know, in a quarter-wavelength stack (one-dimensional photonic crystal), standing wave patterns (defect modes) form at resonant wavelengths when defect layers are present. By tuning the thicknesses and positions of photoconductive layers optimally with respect to the modal overlap with the defect modes, each photoconductive layer will selectively absorb only one specific resonant wavelength. Besides multispectral capability, the proposed design features enhanced optical absorption due to the RCE effect and allows the use of thinner photoconductive layers which significantly reduces shot noise and improves the performance of photoconductive detectors.

In our designed structure schematically shown in Fig. 1(a), the cavity itself is a symmetric mirror stack made up of alternating dielectric layers of SiO_2 ($n=1.45$) and Si-rich Si_3N_4 ($n=2.26$). Si-rich Si_3N_4 instead of stoichiometric Si_3N_4 is used in the stack design in order to maximize the stack refractive index contrast, and thus a large photonic band gap is obtained. Three amorphous Si layers sandwiched between two mirror stacks are separated by two SiO_2 defect layers. The first two of these three amorphous Si layers are connectorized independently to provide dual-wavelength detection. The use of amorphous Si reduces fabrication cost and simplifies device processing by eliminating the complicated single crystal growth process. Meanwhile, amorphous Si exhibits higher absorption compared to its crystalline counterpart in the wavelength range we investigated.

The detector pixels were fabricated through the following procedure: the whole photonic crystal stack was deposited on a (100) Si substrate using plasma enhanced chemical vapor deposition at 400 °C for SiO_2 and Si-rich Si_3N_4 and at 350 °C for amorphous Si, followed by two patterning and plasma etching processes to expose the photoconductive layers. Finally, Al–Si pads were sputtered and patterned to form ohmic contacts through windows opened in the electrically insulating oxide layer. A front view of the device schematic is shown in Fig. 1(a). Importantly, our entire fabrication process is compatible with standard complementary metal oxide semiconductor processing, which projects significant cost reduction for mass production. In order to verify the quality of the stack layers a high resolution cross-section transmission electron microscope (TEM) image of the preprocessed structure was taken and is shown in Fig. 1(b), in which bottom SiO_2/Si-rich Si_3N_4 mirror stack layers as well as three thin amorphous Si layers with uniform thicknesses and smooth interfaces can be seen clearly.

Based on the multispectral concept, we optimized the stack design so as to maximize the detectivity (D^*) as well as minimize the cross-talk between the two preselected wavelength bands. Our optimized detector design was sensitive to 632 and 728 nm wavelengths, as represented by the two resonant peaks in the simulated stack reflectance spectrum in Fig. 2. The experimental reflectance spectrum of the photonic crystal stack measured using a Cary 5E UV–vis–near infrared region dual-beam spectrophotometer shows a very

[a]Electronic mail: anu@mit.edu

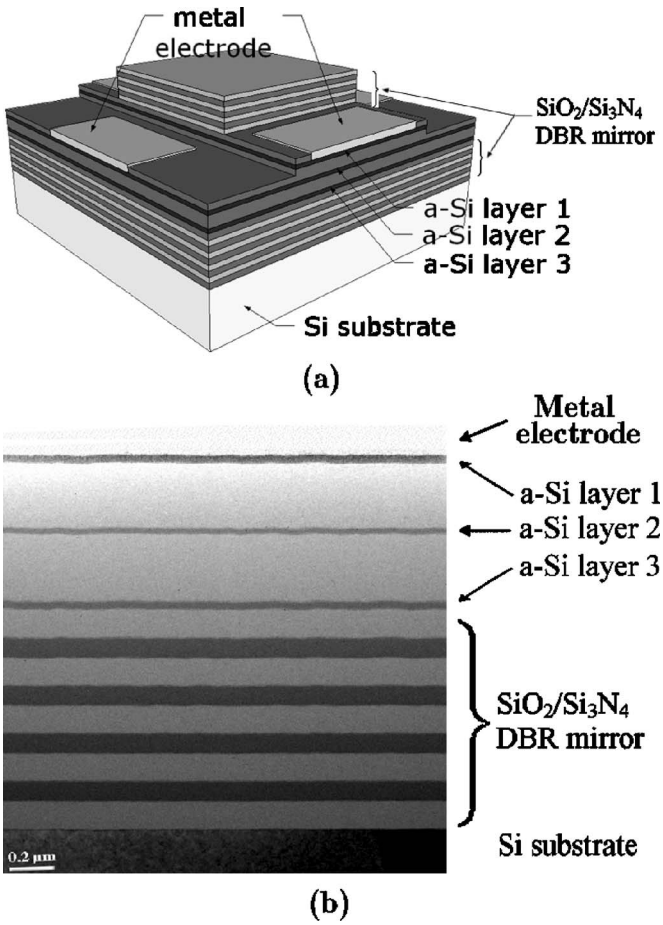

FIG. 1. (a) Design schematic of the dual-wavelength amorphous Si detector. The high-reflectivity mirrors are comprised of alternating layers of SiO_2 and Si-rich Si_3N_4. Three amorphous Si layers are sandwiched between the two mirrors and are separated by two SiO_2 defect layers. Two pairs of metal electrodes connectorize the two amorphous Si layers. Each of the two photoconductive layers is sensitive to one single wavelength band. (b) High resolution cross-section TEM image of a photonic crystal pixel showing the excellent thickness uniformity and smooth interfaces of the photonic crystal stack.

good match with the simulation result, which indicates excellent thickness and refractive index control during the film deposition process.

The fabricated device was electrically characterized using an HP4145A semiconductor parameter analyzer. A fixed voltage (10 V) was applied to the photoconductor and the output current was monitored. A halogen lamp coupled with a Jobin Yvon (Division D Instruments SA) grating monochromator controlled by Optical Science Prop-11 wavelength scanner was used as the light source. Selective multispectral response was observed at resonance wavelength where only one photoconductive layer exhibited photocurrent. Detectivities were calculated using the following equation:

$$D^* = \frac{\sqrt{AB}}{\mathrm{NEP}}, \tag{1}$$

where, A is the detector area, B is the signal bandwidth, and NEP is the noise equivalent power. The dominant noise source, shot noise was used to calculate NEP because high resistance ($>10^{10}$ Ohm) of the thin amorphous Si layers dramatically decreases Johnson noise. As can be seen in Fig. 3, detectivities as high as 2.6×10^{10} cm $\mathrm{Hz}^{1/2}$ W^{-1} at ~632 nm and 2.0×10^{10} cm $\mathrm{Hz}^{1/2}$ W^{-1} at ~728 nm were obtained for

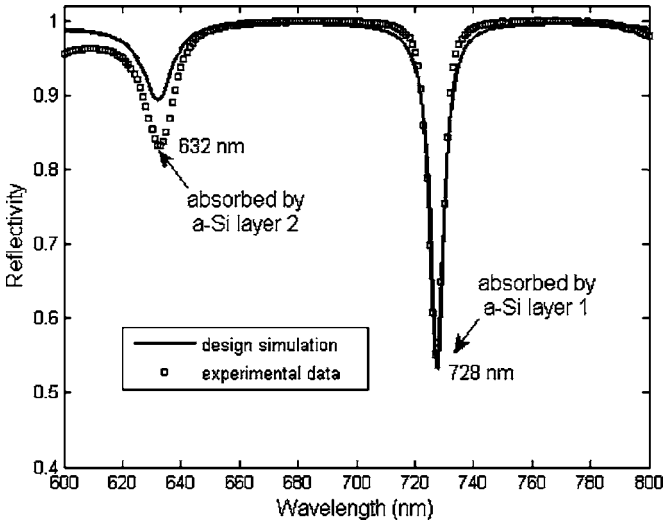

FIG. 2. Experimental data and transfer matrix simulation result of the photonic crystal stack reflectivity showing two resonant absorption peaks at 632 and 728 nm, which are selectively absorbed by the first two of the three amorphous Si layers.

the amorphous Si layer 2 and layer 1, respectively. The measured resonance absorption peaks are significantly broadened due to two major effects. The various incidence angles of noncollimated light through an optical lens shift resonant peaks so as to increase the absorption peak bandwidth. The other effect is the fairly broad bandwidth of the incident light when the grating monochromator slit is tuned to be wider to enhance the incident optical flux. Given the amorphous nature of the photoconductors and the unoptimized electrode pad spacing, these detectivity figures compare favorably to state-of-the-art commercial photodiodes made of single-crystalline Si, which feature a detectivity of $\sim10^{11}$ cm $\mathrm{Hz}^{1/2}$ W^{-1}.

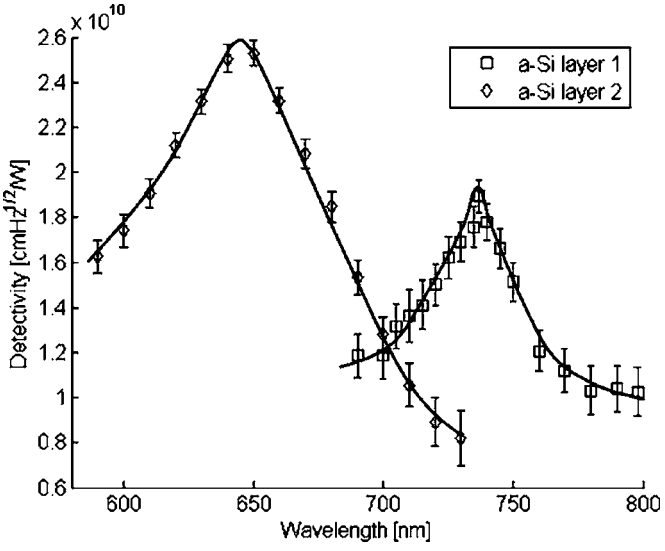

FIG. 3. Detectivity spectra at 10 V of the first two amorphous Si photoconductive layers showing wavelength selectivity. Detectivities are calculated from data measured using a tungsten halogen lamp monochromator. The measured resonance absorption peaks are significantly broadened due to two major effects. The various incidence angles of noncollimated light through an optical lens shift resonant peaks so as to increase the absorption peak bandwidth. The other effect is the fairly broad bandwidth of the incident light when the grating monochromator slit is tuned to be wider to enhance the incident optical flux.

In conclusion, we demonstrate an amorphous Si based photoconductive pixel that utilizes photonic crystal structure for resonance enhancement and multispectrality. Wavelength-selective absorption based on mode discrimination is achieved, and excellent agreement between theory and experiment is demonstrated. The detector shows detectivities as high as $2.6\times10^{10}\,\mathrm{cm\,Hz^{1/2}\,W^{-1}}$ at ~632 nm and $2.0\times10^{10}\,\mathrm{cm\,Hz^{1/2}\,W^{-1}}$ at ~728 nm, corresponding to two resonant modes in the photonic crystal structure.

This work is supported by the Deshpande Center for Technological Innovation at MIT and MIT Lincoln Laboratories. The authors acknowledge the Microsystems Technology Laboratories at MIT and the Center for Materials Science at MIT for fabrication and characterization facilities.

[1] J. Albertz, H. Ebner, and G. Neukum, International Archives of Photogrammetry and Remote Sensing, Vienna, Austria, 1996, Vol. 31, Pt. B4, pp. 58–63.
[2] R. Sandau and A. Eckardt, International Archives of Photogrammetry and Remote Sensing, Vienna, Austria, 1996, Vol. 31, pt. B1, pp. 170–175.
[3] S. Baronti, A. Casini, F. Lotti, and S. Porcinai, Appl. Opt. **37**, 1299 (1998).
[4] S. W. Seo, D. L. Geddis, and N. M. Jokerst, IEEE Photonics Technol. Lett. **15**, 578 (2003).
[5] D. Krapf, B. Adoram, J. Shappir, A. Saar, S. G. Thomas, J. L. Liu, and K. L. Wang, Appl. Phys. Lett. **78**, 495 (2001).
[6] A. Goldberg, S. Kennerly, J. Little, T. Shafer, C. Mears, H. Schaake, M. Winn, M. Taylor, and P. Uppal, Opt. Eng. (Bellingham) **42**, 30 (2003).
[7] A. Kock, E. Gornik, G. Abstretier, G. Bhom, M. Walther, and G. Weimann, Appl. Phys. Lett. **60**, 2011 (1992).